

Received 27 October 2023, accepted 7 November 2023, date of publication 13 November 2023,  
date of current version 17 November 2023.

Digital Object Identifier 10.1109/ACCESS.2023.3332292

## RESEARCH ARTICLE

# Automated Diabetic Foot Ulcer Detection and Classification Using Deep Learning

SUNNAM NAGARAJU<sup>1</sup>, KOLLATI VIJAYA KUMAR<sup>2</sup>, B. PRAMEELA RANI<sup>3</sup>, E. LAXMI LYDIA<sup>4</sup>,  
MOHAMAD KHAIRI ISHAK<sup>5,6</sup>, IMEN FILALI<sup>7</sup>, FATEN KHALID KARIM<sup>7</sup>,  
AND SAMIH M. MOSTAFA<sup>8</sup>

<sup>1</sup>Department of Mechanical Engineering, MLR Institute of Technology, Hyderabad 500043, India

<sup>2</sup>Department of Computer Science and Engineering, GITAM School of Technology, Vishakhapatnam Campus, GITAM (Deemed to be a University),  
Visakhapatnam 530045, India

<sup>3</sup>Department of CSE-AIML, Aditya College of Engineering, Surampalem, Andhra Pradesh 533437, India

<sup>4</sup>Department of Computer Science and Engineering, Vignan's Institute of Information Technology, Visakhapatnam 530049, India

<sup>5</sup>Department of Electrical and Computer Engineering, College of Engineering and Information Technology, Ajman University, Ajman, United Arab Emirates

<sup>6</sup>School of Electrical and Electronic Engineering, Universiti Sains Malaysia, Engineering Campus, Nibong Tebal, Pulau Pinang 14300, Malaysia

<sup>7</sup>Department of Computer Sciences, College of Computer and Information Sciences, Princess Nourah Bint Abdulrahman University, Riyadh 11671, Saudi Arabia

<sup>8</sup>Computer Science Department, Faculty of Computers and Information, South Valley University, Qena 83523, Egypt

Corresponding author: Samih M. Mostafa (samih\_montser@sci.svu.edu.eg)

This work was supported by Princess Nourah bint Abdulrahman University Researchers Supporting Project number (PNURSP2023R300),  
Princess Nourah bint Abdulrahman University, Riyadh, Saudi Arabia.

**ABSTRACT** Diabetic foot ulcers (DFU) are a common and serious complication in individuals with diabetes, and early detection plays a crucial role in effective treatment and prevention of further complications. Automated DFU Detection and Classification using Deep learning (DL) refers to the application of deep learning techniques to automatically detect and classify diabetic foot ulcers from medical images. DL, a subfield of machine learning, has shown promising results in medical imaging analysis, including diabetic foot ulcer detection. The use of deep learning in DFU detection provides various benefits, including the ability to learn complex features, adaptability to different image modalities, and the potential for high accuracy in detection and classification tasks. Therefore, this article introduces a novel sparrow search optimization (SSO) with deep learning enabled diabetic foot ulcer detection and classification (SSODL-DFUDC) technique. The presented SSODL-DFUDC technique's goal lies in identifying and classifying DFU. The proposed technique employs the Inception-ResNet-v2 model for feature vector generation to accomplish this. Since the trial and error manual hyperparameter tuning of the Inception-ResNet-v2 model is a tedious and erroneous process, the SSO algorithm can be used for the optimal hyperparameter selection of the Inception-ResNet-v2 model which in turn enhances the overall DFU classification results. Moreover, the classification of DFU takes place using the stacked sparse autoencoder (SSAE) model. The comprehensive experimental outcomes demonstrate the improved performance of the SSODL-DFUDC system related to existing DL techniques.

**INDEX TERMS** Medical image analysis, deep learning, diabetic foot ulcer, sparrow search optimization, computer-aided diagnosis.

## I. INTRODUCTION

Amputation of the limb or foot may be caused by a diabetic foot ulcer (DFU) infection. The probability of survival can be lesser for patients having amputated limbs [1]. It damages the

The associate editor coordinating the review of this manuscript and approving it for publication was Bijoy Chand Chatterjee.

livelihood of quality and distresses social participation and the outcome of these causes and tissue death because of diseases. The DFU is increasing rapidly. Because of the scarcity of specialists and lack of resources in the medication for diabetic foot ulcers, over a million diabetic patients at higher risk of diabetic Mellitus will lose out foot (partly) every year [2]. Notably, for every 20 seconds, one diabetic foot functioned.

A complete study of medical data was essential for specialists to accomplish a precise outcome [3]. Conventional diagnostic techniques were labour-intensive and vulnerable to human errors. The computer-based diagnostic process's utility includes minimal performance enhancement [4]. Current advancements in n wearable and mobile health gadgets help in controlling diabetes and its limitations, improving the standards of life and extending remission for patients by s controlling harmful sensing and foot pressure and inflammation [5]. The development of novel-generation medical sensors recommends expanding such devices' utility in the medical field [6]. In the contemporary healthcare mechanism, medical images are used for diagnosing several patient difficulties [7].

Conventional approaches for analysis of DFU use hand-crafted rendered technique [8]. However, research activities in the publication have displayed that learned attributes by deep neural networks (DNN) have high potential compared to classical hand-crafted features [9]. Wide research was conducted to enhance the outcome of computerized are very popular in this sector since they were superior to other techniques [10]. The common method that is utilized in the DL technique in medical image classification is convolutional neural networks (CNNs). The CNNs can efficiently derive valuable attributes for image segmentation, image classification, other vision tasks, and object detection [11]. With the obtainability of large-scale trained data and high-performing modern application specific integrated circuit (ASICs) and graphics processing units (GPUs) and techniques related to CNNs have enhanced the precision of image classification. Renowned CNNs for general image classifier tasks involve ResNet, AlexNet, EfficientNet, and VGG [12]. Such networks generally serve as the pillar of medical image classifier networks or directly enforce medical image classifications by transfer learning (TL) with pre-trained variables on large-scale datasets (e.g., ImageNet). Practically, labelling and collecting medical images were costly [13]. TL was a potential way to overcome the need for medicinal trained data.

This article introduces a novel sparrow search optimization with deep learning enabled diabetic foot ulcer detection and classification (SSODL-DFUDC) technique. The goal of this technique lies in the identification and classification of DFU. To perform this task, the SSODL-DFUDC technique employs the Inception-ResNet-v2 model for feature vector generation and utilizes the SSO algorithm for hyperparameter tuning. The SSAE model is used for DFU data set classification.

The rest of the paper is organized as follows. Section II provides the related works and section III offers the proposed model. Then, section IV gives the result analysis and section V concludes the paper.

## II. LITERATURE REVIEW

Cassidy et al. [14] present a mobile and cloud-based structure for the automatic recognition of DFUs and perform an anal-

ysis of its efficiency. This method utilizes a cross-platform mobile structure which allows the utilization of mobile applications for several environments utilizing a single TypeScript code base. A DCNN has been used in a cloud-based environment, but the mobile application sends photographs of patients' feet to inference for detecting the occurrence of DFUs. Munadi et al. [15] present a new structure for the DFU classifier dependent upon thermal imaging utilizing DNNs and decision fusion. At this point, decision fusion integrates the classifier outcome in a parallel classification. The author utilized the CNN technique of MobileNetV2 and ShuffleNet as the baseline classification. In evolving the classification process, initially, the ShuffleNet and MobileNetV2 can be trained to utilize plantar thermogram databases.

Alshayegi and Sindhu's [16] investigation is new since, without any prior analysis utilized typical ML techniques for the analysis of DFU in the thermal image and also did not utilize SURF, BOF, or SIFT approaches. Also, the authors utilize direct temperature files of all feet and then map them on images to obtain the correct temperature distribution. Typical ML techniques are chosen in the last step to binary classifier betwixt normal and DFU. D'Angelo et al. [17] examine a method dependent upon Genetic Programming (GP) for creating an easy global explainable classifier termed X-GPC that different present tools, like SHAP and LIME, offer a global analysis of DFU with the mathematical process. Moreover, the medicinal clinical staff was offered a simple consultable 3D graph that is utilised to understand the patient's condition and make decisions for patient recovery. In [18], a new Deep CNN, DFU\_QUTNet, is also presented for the automatic classifier of normal skin (healthy skin) towards abnormal skin (DFU) classes. Stacking further layers to a classic CNN to arrive very deep could not cause optimum efficacy, resulting in worse execution because of the gradient.

Goyal [19] progressed automatic computer vision (CV) schemes which recognize the DFU of distinct grades and steps. Primarily, the authors utilized ML techniques for classifying the DFU spots against normal skin spots of the foot area to determine the feasible misclassified reasons for both classes. Secondly, the authors utilized FCN for the segmentation of DFU and neighbouring skin from entire foot images. Lastly, the authors utilized robust and lightweight deep localization schemes from mobile devices for detecting the DFU on foot image to a remote monitor. In [20], a novel image processing system was presented for effectual calculation and classifier of DFU images. Primarily, pre-processed was completed by cascaded fuzzy filter and then non-linear partial differential equation (NPDE) based segmentation which segmented the foot ulcer areas. Accordingly, the LBP was utilized for extracting the valuable features. Afterwards, the presented hybrid GWO-CNN technique utilizes these features for identifying the DFU areas. In [21], a unique stacked parallel convolutional layer-based network (DFU\_SPNet) was presented for performing DFU versus normal skin classification.

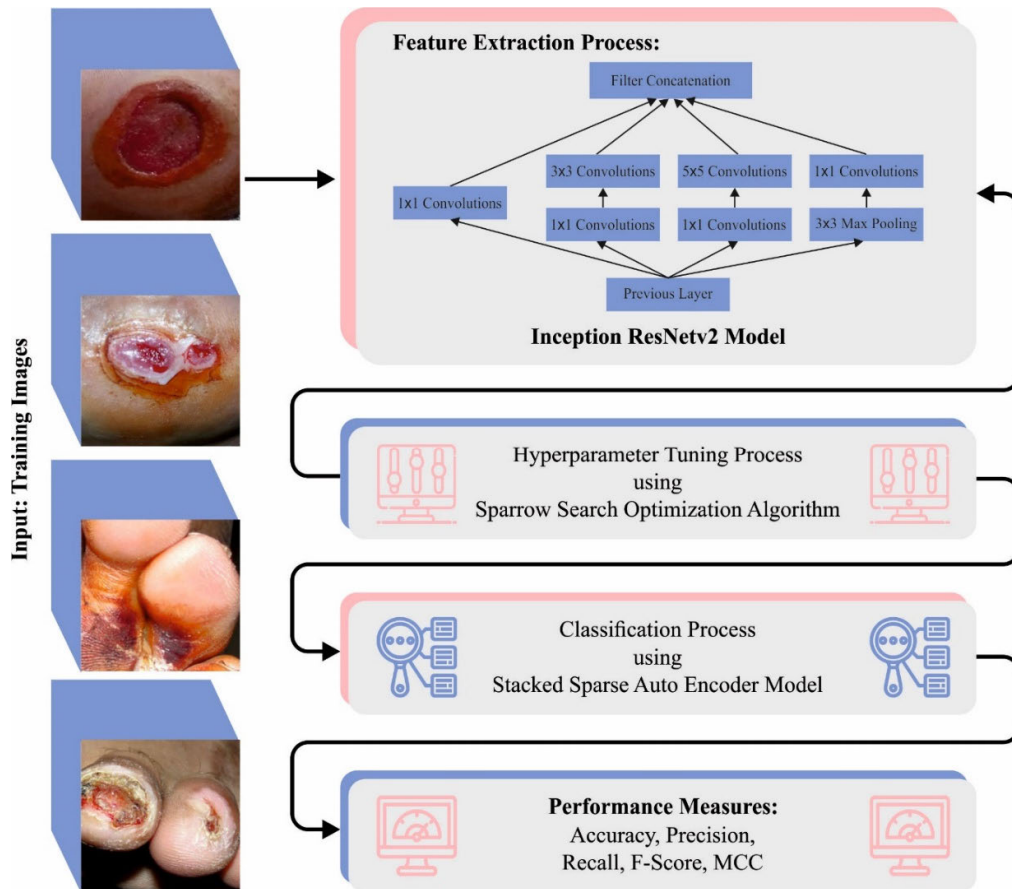


FIGURE 1. Workflow of SSODL-DFUDC approach.

In [22], a pre-training ResNet-50 approach and altered classical-quantum approach can be employed for DFU classification as equivalent class labels like ischaemia/non-ischaemia and normal/abnormal. Al-Garaawi et al. [23] examine a CNN-based DFU classification approach where it can be demonstrated that feeding a suitable feature to the CNN technique offers a complementary efficiency to typical RGB-based deep approaches of DFU classification tasks and the optimum solution was attained when either RGB images or their texture features can be integrated and utilized as input to CNN. da Costa Oliveira et al. [24] present the utilisation of DL approaches to help in the cure of DFUs. In detail, the recognition of ulcers by photos taken in the patient feet. The authors present a development of Faster R-CNN utilizing data augmentation approaches and modifications in parameter settings. Venkatesan et al. [25] aimed to develop and design a novel lightweight CNN approach to analyse NFU termed as NFU-Net.

Huang et al. [26] present an endwise ViT-AMC network (ViT-AMCNet) with adaptive model fusion and multi-objective optimizer which combines and fuses the ViT and AMC blocks. Zhou et al. [27] examine an adaptive sparse interaction ResNet-ViT dual-branch network (ASI-DBNet). Initially, the authors plan the ResNet-ViT parallel infrastruc-

ture for simultaneously capturing and retaining the local and global data of pathology images. Huang et al. [28] introduce an endwise depth domain adaptive network (DDANet) with a combination gradient CAM and priori experience-guided attention for improving the tumour grading solution and interpretability by presenting the pathologist's previous experience in high-magnification as depth model. Zhou et al. [29] developed a laryngeal cancer classification network (LPCANet) that relies on a CNN and attention mechanisms. Primary, the original histopathological images can be sequentially cropped as patches. Huang et al. [30] introduce a novel fusion attention block network (FABNet) for addressing these issues.

### III. THE PROPOSED MODEL

In this article, we have developed a new SSODL-DFUDC technique to detect and classify DFU. The presented SSODL-DFUDC technique's goal lies in identifying and classifying DFU. Fig. 1 represents the workflow of the SSODL-DFUDC algorithm. The figure indicates that the presented SSODL-DFUDC technique follows three major processes: Inception-ResNet-v2 feature extraction, SSO-based hyperparameter tuning, and SSAE classification.

**A. FEATURE EXTRACTION USING OPTIMAL DL MODEL**

The presented SSODL-DFUDC technique employed the Inception-ResNet-v2 model for feature vector generation. CNN is the algorithm of the DL algorithm. CNN is a progression of MLP developed for processing the dataset in grid form [31]. CNN is exploited on the image dataset. The objective of the training model is to train the ANN module to reduce the error of predictive results of the model with the original dataset. The convolutional layer is a convolutional operation between two vectors. In Eq. (1), it is convolutional of two functions where  $g(x)$  is named the convolutional kernel (filter) that is functioned in shifts on the vector  $F(x)$ .

$$h(x) = F(x) \cdot g(x) = \int F(a) \cdot g(x - a) \quad (1)$$

CNN comprises two phases. Initially, group images with feedforward. Then, use the backpropagation algorithm. Currently, the wrapping and cropping systems are performed to emphasize the categorised object before doing the classification. Next, training can be done by backpropagation and feed-forward techniques. The structure of CNN is split into two most important parts, such as the Fully-Connected Layer and Feature Extraction Layer. Inception-ResNetV2 is a CNN architecture trained originally on the ImageNet datasets, comprising 164 layers. The model has learned feature representation and is stronger for a large number of image types. This model accepts the input of  $299 \times 299$  and the hybridization of two currently established networks, the modern architectural version, and residual links. There are sequences of filters, namely  $1 \times 1$ ,  $3 \times 3$ ,  $5 \times 5$ , and so on, merged with all the branch concatenation. The split-transformation-mixing architecture of the initiation model is perceived in its thick layer as a stronger representation. The residual connection enables the training of progressively DNN, leading to remarkable performance. This model was trained and fine-tuned through TL in this work.

**TABLE 1. Details of dataset.**

Class	No. of Images
Abnormal	410
Normal	434
<b>Total Number of Images</b>	<b>844</b>

In this work, the SSODL-DFUDC technique utilizes the SSO algorithm for hyperparameter tuning. The SSO is a recent heuristic approach inspired by the behaviours of sparrows foraging and avoiding predators and characteristics of group socialization [32]. The SSO benefits from strong optimization ability, simple architecture, easier implementation, few control parameters, and so on. The SSO to converge to the present optimum solution is to jump towards the existing ideal solution's locality directly. Hence the SSO technique is better than the particle swarm optimization, grey wolf optimization, and gravity search algorithms with respect to robustness, accuracy, convergence speed, and stability.



**FIGURE 2. Sample images a) Normal (Healthy) b) Abnormal (Ulcer).**

In this work, sparrows are alienated into vigilant and discoverer followers. The location of every sparrow corresponds to the solution. The position of each sparrow in the sparrow groups is characterized as  $X$  matrix:

$$X = \begin{pmatrix} x_{1,1} & \dots & x_{1,d} \\ \vdots & \dots & \vdots \\ x_{m,1} & \dots & x_{m,d} \end{pmatrix} \quad (2)$$

In Eq. (10),  $m$  indicates the count of sparrows, and  $d$  denotes the dimension of the variable that is enhanced. The fitness function (FF) corresponds to all the sparrows are characterized as an  $F$  matrix:

$$F = \begin{pmatrix} f([x_{1,1} \dots x_{1,d}]) \\ \vdots \\ f([x_{m,1} \dots x_{m,d}]) \end{pmatrix} \quad (3)$$

where  $f([x_{i,1}, \dots, x_{i,d}])$  signifies the fitness value of  $i$ -th sparrows. In all the iterations, the position of discoverer will be upgraded, as follows:

$$X_{ij}^{t+1} = \begin{cases} x_{ij}^t \cdot \exp\left(\frac{-i}{\alpha \cdot N}\right), & \text{if } R_2 < ST \\ x_{ij}^t + Q \cdot L, & \text{if } R_2 \geq ST \end{cases} \quad (4)$$

where  $t$  signifies the existing amount of iterations, and  $N$  signifies the maximum amount.  $\alpha$  indicates a random integer, and  $\alpha \in (0, 1]$ .  $R_2$  characterizes the alarm value that is an arbitrary integer, and  $R_2 \in [0, 1][0, 1]$ .  $ST$  signifies the safety threshold and  $ST \in [0.5, 1.0]$ .  $Q$  shows the random number subjected to the standard distribution, and  $L$  represents the row vector whose element is equivalent to 1. The updating rules of the follower are shown below:

$$X_{ij}^{t+1} = \begin{cases} Q \cdot \exp\left(\frac{X_W^t - X_{IJ}^t}{i^2}\right), & \text{if } i > \frac{n}{2} \\ x_{ij}^{t+1} + |X_{ij}^t - x_{DB}^{t+1}| \cdot M' \cdot L, & \text{if } i \leq \frac{n}{2} \end{cases} \quad (5)$$

In Eq. (5)  $X_W^t$  signifies the worst location of the  $t$ -th iteration, and  $x_{DB}^{t+1}$  signifies the location of finders with maximum fitness value at the  $t + 1$  iteration.  $M$  signifies the  $1 \times d$

**TABLE 2. Classifier outcome of SSDL-DFUDC approach with distinct measures and folds.**

Class	Accuracy <sub>bal</sub>	Precision	Recall	F-Score	AUC Score	MCC
<b>Fold - 1</b>						
Abnormal	99.02	99.27	99.02	99.15	99.17	98.34
Normal	99.31	99.08	99.31	99.19	99.17	98.34
<b>Average</b>	<b>99.17</b>	<b>99.17</b>	<b>99.17</b>	<b>99.17</b>	<b>99.17</b>	<b>98.34</b>
<b>Fold - 2</b>						
Abnormal	98.78	99.26	98.78	99.02	99.04	98.10
Normal	99.31	98.85	99.31	99.08	99.04	98.10
<b>Average</b>	<b>99.04</b>	<b>99.06</b>	<b>99.04</b>	<b>99.05</b>	<b>99.04</b>	<b>98.10</b>
<b>Fold - 3</b>						
Abnormal	98.78	99.26	98.78	99.02	99.04	98.10
Normal	99.31	98.85	99.31	99.08	99.04	98.10
<b>Average</b>	<b>99.04</b>	<b>99.06</b>	<b>99.04</b>	<b>99.05</b>	<b>99.04</b>	<b>98.10</b>
<b>Fold - 4</b>						
Abnormal	99.02	99.27	99.02	99.15	99.17	98.34
Normal	99.31	99.08	99.31	99.19	99.17	98.34
<b>Average</b>	<b>99.17</b>	<b>99.17</b>	<b>99.17</b>	<b>99.17</b>	<b>99.17</b>	<b>98.34</b>
<b>Fold - 5</b>						
Abnormal	99.02	99.27	99.02	99.15	99.17	98.34
Normal	99.31	99.08	99.31	99.19	99.17	98.34
<b>Average</b>	<b>99.17</b>	<b>99.17</b>	<b>99.17</b>	<b>99.17</b>	<b>99.17</b>	<b>98.34</b>
<b>Fold - 6</b>						
Abnormal	99.02	99.27	99.02	99.15	99.17	98.34
Normal	99.31	99.08	99.31	99.19	99.17	98.34
<b>Average</b>	<b>99.17</b>	<b>99.17</b>	<b>99.17</b>	<b>99.17</b>	<b>99.17</b>	<b>98.34</b>
<b>Fold - 7</b>						
Abnormal	98.78	99.26	98.78	99.02	99.04	98.10
Normal	99.31	98.85	99.31	99.08	99.04	98.10
<b>Average</b>	<b>99.04</b>	<b>99.06</b>	<b>99.04</b>	<b>99.05</b>	<b>99.04</b>	<b>98.10</b>
<b>Fold - 8</b>						
Abnormal	99.27	99.27	99.27	99.27	99.29	98.58
Normal	99.31	99.31	99.31	99.31	99.29	98.58
<b>Average</b>	<b>99.29</b>	<b>99.29</b>	<b>99.29</b>	<b>99.29</b>	<b>99.29</b>	<b>98.58</b>
<b>Fold - 9</b>						
Abnormal	99.02	99.27	99.02	99.15	99.17	98.34
Normal	99.31	99.08	99.31	99.19	99.17	98.34
<b>Average</b>	<b>99.17</b>	<b>99.17</b>	<b>99.17</b>	<b>99.17</b>	<b>99.17</b>	<b>98.34</b>
<b>Fold - 10</b>						
Abnormal	98.78	96.20	98.78	97.47	97.55	95.06
Normal	96.31	98.82	96.31	97.55	97.55	95.06
<b>Average</b>	<b>97.55</b>	<b>97.51</b>	<b>97.55</b>	<b>97.51</b>	<b>97.55</b>	<b>95.06</b>

matrix where the element is randomly fixed to 1 or -1.  $M' = M^T(M \cdot M^T)^{-1}$ , and  $M^T$  implies the matrix was transposed. The position updating of vigilant is:

$$X_{i,j}^{t+1} = \begin{cases} x_{GB}^t + \gamma \cdot \left| X_{ij}^t - x_{GB}^t \right|, & \text{if } f_i \neq f_B \\ x_{GB}^t + k \cdot \left( \frac{X_{i,j}^t - x_{GB}^t}{|f_i - f_w| + \varepsilon} \right), & \text{if } f_i = f_B \end{cases} \quad (6)$$

In Eq. (6),  $x_{GB}^t$  signifies the global optimum position at the  $t$ -th iteration,  $\gamma$  indicates the control step size, and  $\gamma \sim N(0, 1)$ .  $k$  shows the random value and  $k \in [-1, 1]$ , while  $\varepsilon$  indicates the constant that rises to avoid the denominator from being.  $f_i$  indicates the fitness value of  $i$ -th sparrows, whereas  $f_B$  and  $f_w$  signify the fitness values of global optimum and worst sparrows, correspondingly. The superparameters that the SSO could alter include the safety value  $ST$ , the maximal amount of iterations  $N$ , and  $n$ , the number of sparrows. Furthermore, there are upper and lower bounds of the independent parameter  $DL$ , several discoveries  $PD$ , and the number of vigilantes  $SD$ . The independent parameter's dimension is determined by the number of network layers and the input vector.

The fitness selection can be a vital element in the SSO method. Solution encoding can be used to evaluate the goodness of the candidate solution. The accuracy value was the main condition used to devise an FF.

$$Fitness = \max(P) \quad (7)$$

$$P = \frac{TP}{TP + FP} \quad (8)$$

From the expression, TP represents the true positive, and FP denotes the false positive value.

**B. DFU CLASSIFICATION USING THE SSAE MODEL**

In this study, the classification of DFU takes place using the SSAE model. Hinton, in 2006, proposed an Autoencoder (AE) paradigm of ANN, and it is extensively used in reduction dimensionality [33]. The primary objective is to train the model with a similar input and output dataset. The architecture of the AE network contains a hidden layer (HL) with  $m$  neurons, an input layer with  $n$  neurons, and an output layer with  $n$  neurons. Firstly, the  $n$ -dimension sample is mapped from the input to the hidden layers that characterize an encoding method of  $h_{w1,b1}(x) \in R^m$ . Following,

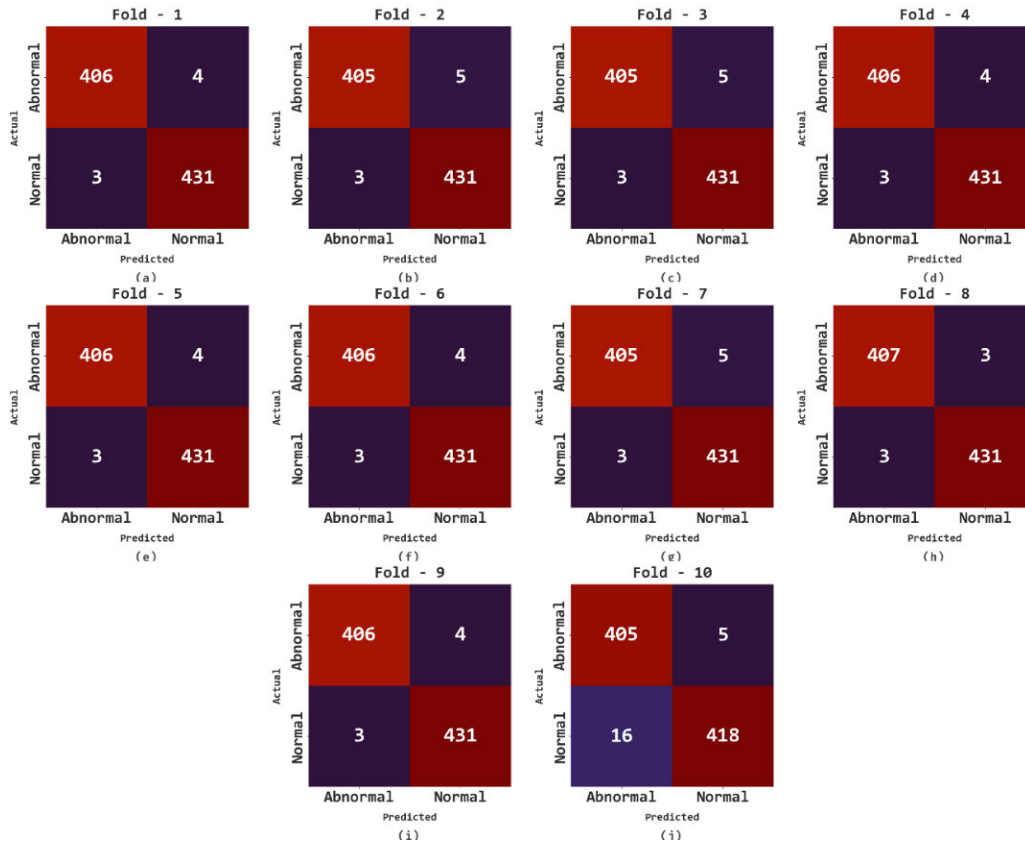


FIGURE 3. Confusion matrices of SSODL-DFUDC approach (a-j) Fold 1-10.

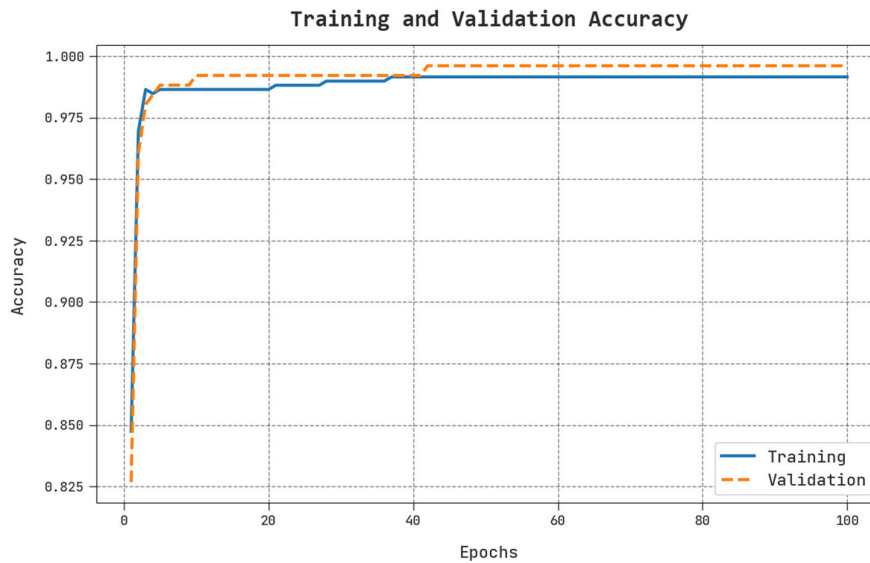


FIGURE 4. TACC and VACC analysis of the SSODL-DFUDC system.

$h_{w1,b1}(x)$  is decoded from the HL and mapped back to the  $n$ -dimensional space  $R^n$  to recreate the input. The training process of the AE network is to perform the backpropagation of error and continuously upgrade the network parameter for making the  $\tilde{x}$  output to the  $x$  input, where  $\tilde{x} = h_{w,b}(x)$ . The

loss function of the AE network can be determined by:

$$J_{AE}(W, b) = \frac{1}{N} \sum_{i=1}^m \left( \frac{1}{2} \|\tilde{x} - x\|_2^2 \right) + \frac{\lambda}{2} \sum_{j=1}^2 \|W_j\|_2^2 \quad (9)$$

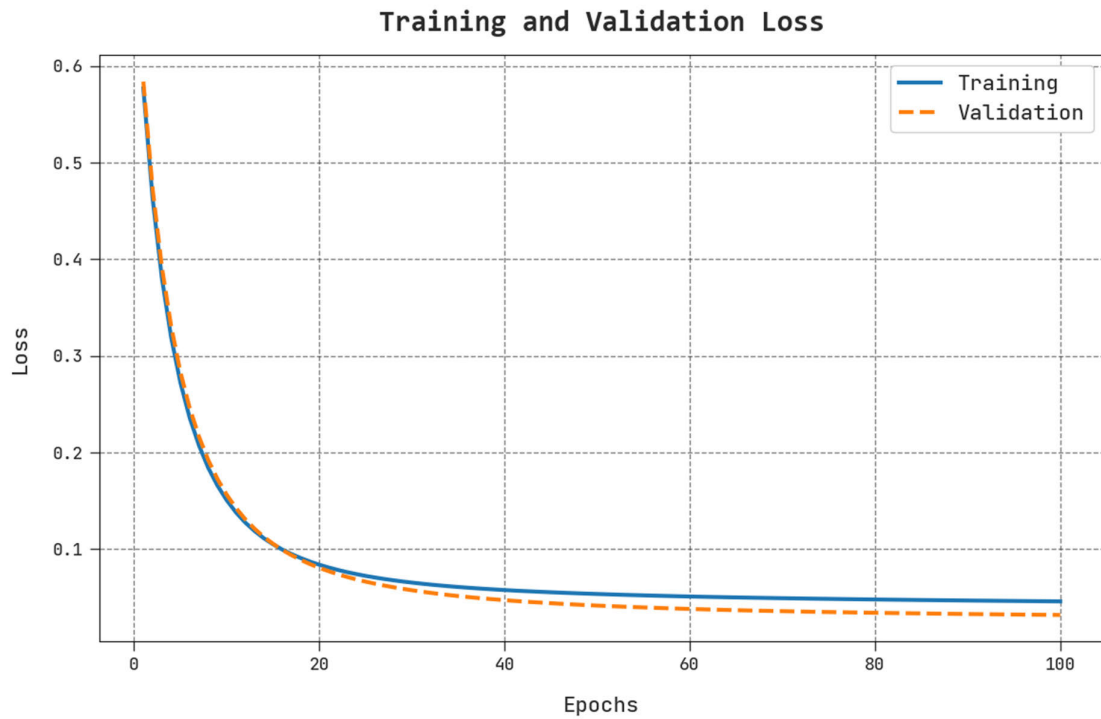


FIGURE 5. TLS and VLS analysis of SSODL-DFUDC system.

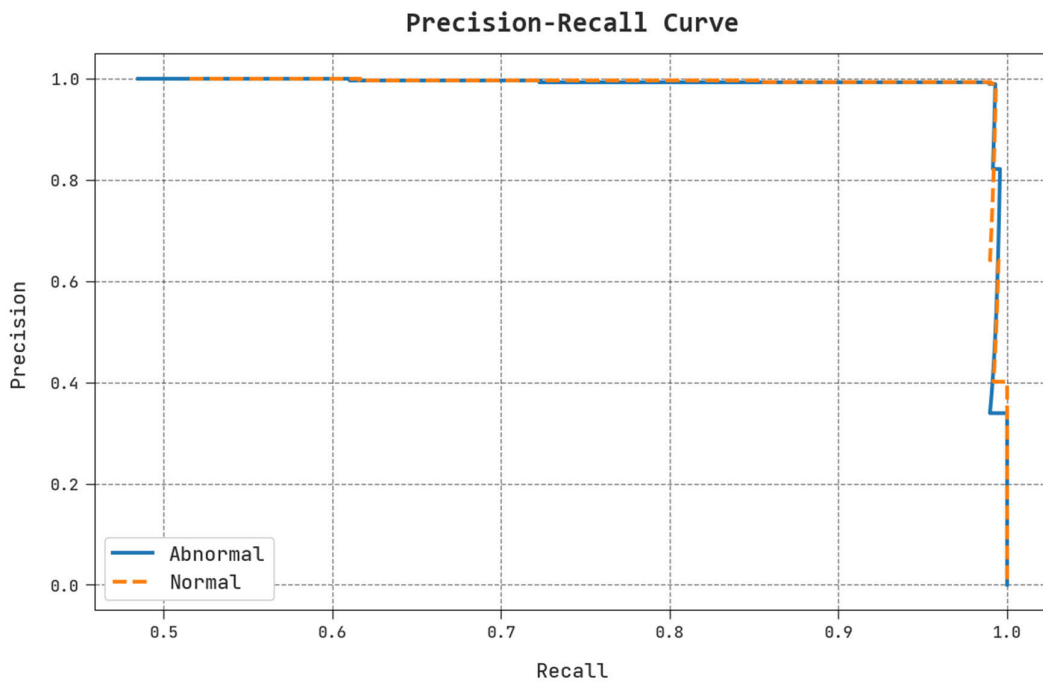


FIGURE 6. Precision-recall analysis of SSODL-DFUDC system.

where  $J_{AE}(W, b)$  indicates the loss function of the AE network,  $x$  denotes the input of the network,  $\tilde{x}$  shows the output of the network,  $N$  represents the overall amount of input samples,  $\|W_j\|_2^2$  shows the regularization,  $W_j$  indicates the

weight matrices between  $j^{th}$  layers and the next layer, and  $\lambda$  denotes the weight of regularization. Once the amount of HL nodes is lesser than the input layer, the output of HL is regarded as a new feature extracted to accomplish

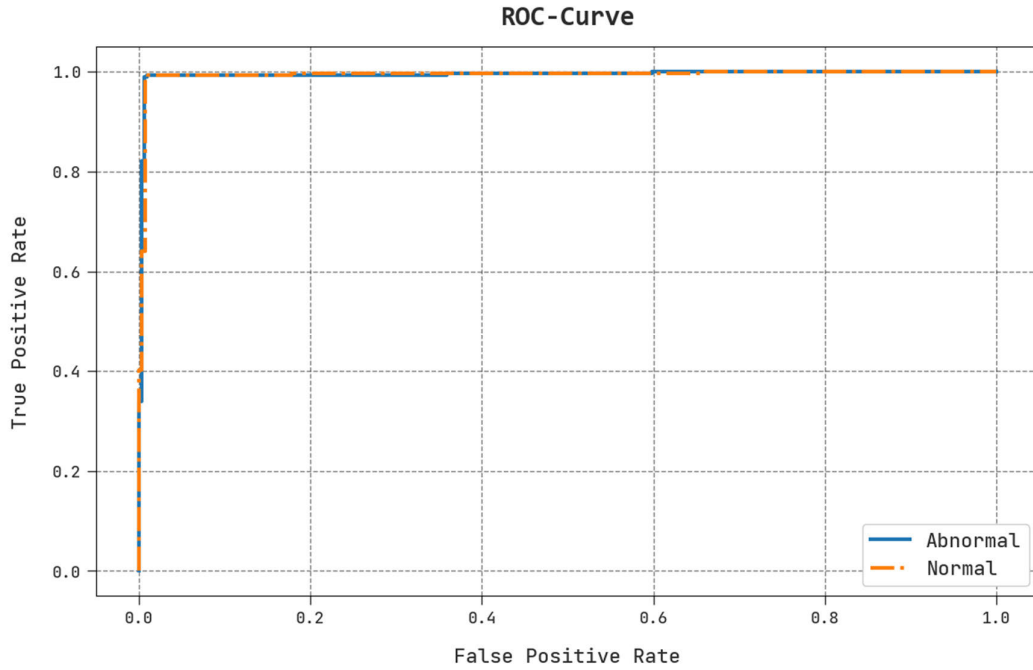


FIGURE 7. ROC analysis of the SSODL-DFUDC system.

reduction dimensionality. Once the amount of HL nodes is larger, a sparse autoencoder (SAE) is adopted. To avoid overfitting, SAE added sparsity limitation to the AE network and exploited the sigmoid function as an activation function that inhibits the neuron in the hidden layer. The suppressed state implies that the neuron output is closer to zero. For the input  $x$ , the activation degree of  $j^{\text{th}}$  neurons in the HL is  $h_j(x)$ , then the average activation degree of these neurons in the entire training samples  $S = \{x_{(i)}\}_{i=1}^N$  is  $\hat{\rho}_j = \frac{1}{N} \sum_{i=1}^N h_j(x_{(i)})$ . To guarantee that the neuron is suppressed, we must make the average activation degree closer to the sparse variable  $\rho$ , which is generally closer to zero. A penalty factor is added to the loss function of AE to accomplish the sparsity. The loss function of the SAE network is formulated by:

$$J_{\text{sparse}}(W, b) = J_{\text{AE}}(W, b) + \beta \sum_{j=1}^J \text{KL}(\rho || \hat{\rho}_j) \quad (10)$$

In Eq. (10),  $\hat{\rho}_j$  indicates the average activation degree of each neuron with every training sample,  $\rho$  denotes the sparse variable to be set.  $\text{KL}(\rho || \hat{\rho}_j)$  represents the relative entropy between  $\rho$  and  $\hat{\rho}_j$ , viz., the KL divergence that value increases monotonically as the difference between  $\rho$  and  $\hat{\rho}_j$ .  $\beta$  denotes the weight of KL divergence. Once  $\rho$  and  $\hat{\rho}_j$  are equivalent, then  $\text{KL}(\rho || \hat{\rho}_j)$  is equivalent to for getting its minimal value. Since  $\rho$  is generally closer to zero,  $\hat{\rho}_j$  of each neuron in the HL would be controlled to be within a smaller range afterwards training, and the sparse representation of the input signal is lastly attained. The SSAE is encompassed by a single-layer SAE network, with the output of SAE of the preceding layer, which acts as an input of SAE of the following adjacent layer. By training the SAE network layer-wise, the SSAE network

could eventually extract the feature concealed in the input for realizing reduction dimensionality.

#### IV. EXPERIMENTAL VALIDATION

In this section, the DFU results of the SSODL-DFUDC technique are tested using a dataset from the Kaggle repository [34]. The dataset includes 844 samples, with 410 abnormal and 434 standard samples, as demonstrated in Table 1. Fig. 2 showcases the sample images of normal and abnormal.

Table 2 represents the overall DFU detection results of the SSODL-DFUDC technique under different folds. The results showed that the SSODL-DFUDC technique has enhanced results under all folds. For instance, with fold-1, the SSODL-DFUDC technique reaches average  $accu_{bal}$ ,  $prec_n$ , and  $reca_l$  of 99.17%, 99.17%, and 99.17%, respectively. Meanwhile, with fold-5, the SSODL-DFUDC system gains average  $accu_{bal}$ ,  $prec_n$ , and  $reca_l$  of 99.17%, 99.17%, and 99.17%, correspondingly. Eventually, with fold-10, the SSODL-DFUDC approach attains average  $accu_{bal}$ ,  $prec_n$ , and  $reca_l$  of 99.55%, 97.51%, and 97.55%, correspondingly.

The TACC and VACC of the SSODL-DFUDC approach are investigated on DFU performance in Fig. 4. The figure pointed out that the SSODL-DFUDC system has shown improved performance with improved values of TACC and VACC. It is perceptible that the SSODL-DFUDC system has reached maximal TACC outcomes.

The classification results of the SSODL-DFUDC technique are inspected in the form of a confusion matrix in Fig. 3. The results implied that the SSODL-DFUDC technique has successfully recognized the presence of normal and abnormal samples.



**TABLE 3.** Comparative analysis of SSODL-DFUDC system with existing algorithms [35].

Methods	Accuracy	Precision	Recall	F1-Score
SSODL-DFUDC	99.29	99.29	99.29	99.29
Inception-ResNet-v2	98.98	98.71	98.68	98.94
AlexNet	92.01	90.93	87.22	88.94
VGG16	97.87	92.21	90.18	90.67
DFUNet-KNN	95.63	93.75	92.39	93.00
DFUNet	96.97	94.17	92.11	92.75
DFUNet-SVM	96.23	95.17	92.86	94.09
GoogleNet	97.12	95.17	90.22	92.85
EfficientNet	98.89	98.64	98.54	99.11

The TLS and VLS of the SSODL-DFUDC method are tested on DFU performance in Fig. 5. The figure states that the SSODL-DFUDC technique has exposed improved performance with the lowest values of TLS and VLS. It is observable that the SSODL-DFUDC model has resulted in reduced VLS outcomes.

An evident precision-recall study of the SSODL-DFUDC methodology in the test database is described in Fig. 6. The figure implied that the SSODL-DFUDC system has led to superior values of precision-recall values in two classes.

A detailed ROC study of the SSODL-DFUDC algorithm in the test database is exposed in Fig. 7. The outcome stated the SSODL-DFUDC system has displayed its capability to classify two class labels.

To illustrate the enhanced performance of the SSODL-DFUDC technique, a widespread comparison study is made in Table 3 and Fig. 8 [35]. The experimental values indicated that the AlexNet model reaches poor performance. At the same time, the DFUNet-KNN, DFUNet, and DFUNet-SVM models have attained slightly enhanced outcomes. Along with that, the VGG16 and GoogleNet models have obtained moderately improved performance. Although the EfficientNet model results in reasonable performance, the SSODL-DFUDC technique outperforms the existing ones with an increased  $accu_y$  of 99.29%,  $prec_n$  of 99.29%,  $reca_l$  of 99.29%, and  $F1_{score}$  of 99.29%. These results assured the improved performance of the SSODL-DFUDC technique in the classification process.

## V. CONCLUSION

In this article, we have developed a novel SSODL-DFUDC system to detect and classify DFU. The presented SSODL-DFUDC technique's goal lies in identifying and classifying DFU. To accomplish this, the presented SSODL-DFUDC technique has applied the Inception-ResNet-v2 model for feature vector generation. In addition, the SSODL-DFUDC technique utilizes the SSO algorithm for hyperparameter tuning purposes. Moreover, the classification of DFU takes place using the SSAE model. The experimental results of the SSODL-DFUDC technique take place using the DFU dataset. The comprehensive experimental outcomes demonstrate

the improved efficiency of the SSODL-DFUDC approach compared to existing DL techniques. In the future, the SSODL-DFUDC algorithm's performance can be improved by advanced DL classification models. In addition, weakly supervised learning techniques can be explored to reduce the dependency on precise pixel-level annotations. Instead of relying solely on expert-labeled ulcer regions, weakly supervised learning can utilize weak labels, such as image-level or bounding box annotations, making it more scalable and easier to collect data.

## ACKNOWLEDGEMENT

Princess Nourah bint Abdulrahman University Researchers Supporting Project number (PNURSP2023R300), Princess Nourah bint Abdulrahman University, Riyadh, Saudi Arabia.

## REFERENCES

- [1] S. Wang, J. Wang, M. X. Zhu, and Q. Tan, "Machine learning for the prediction of minor amputation in university of Texas grade 3 diabetic foot ulcers," *PLoS ONE*, vol. 17, no. 12, Dec. 2022, Art. no. e0278445.
- [2] M. Swerdlow, L. Shin, K. D'Huyvetter, W. J. Mack, and D. G. Armstrong, "Initial clinical experience with a simple, home system for early detection and monitoring of diabetic foot ulcers: The foot selfie," *J. Diabetes Sci. Technol.*, vol. 17, no. 1, pp. 79–88, Jan. 2023.
- [3] M. Goyal, N. D. Reeves, S. Rajbhandari, N. Ahmad, C. Wang, and M. H. Yap, "Recognition of ischaemia and infection in diabetic foot ulcers: Dataset and techniques," *Comput. Biol. Med.*, vol. 117, Feb. 2020, Art. no. 103616.
- [4] J. Yogapriya, V. Chandran, M. G. Sumithra, B. Elakkiya, A. S. Ebenezer, and C. S. G. Dhas, "Automated detection of infection in diabetic foot ulcer images using convolutional neural network," *J. Healthcare Eng.*, vol. 2022, pp. 1–12, Apr. 2022.
- [5] K. S. Chan and Z. J. Lo, "Wound assessment, imaging and monitoring systems in diabetic foot ulcers: A systematic review," *Int. Wound J.*, vol. 17, no. 6, pp. 1909–1923, Dec. 2020.
- [6] B. Cassidy, C. Kendrick, N. D. Reeves, J. M. Pappachan, C. O'Shea, D. G. Armstrong, and M. H. Yap, "Diabetic foot ulcer grand challenge 2021: Evaluation and summary," in *Diabetic Foot Ulcers Grand Challenge*. Cham, Switzerland: Springer, Sep. 2021, pp. 90–105.
- [7] H. Pan, H. Peng, Y. Xing, L. Jiayang, X. Hualiang, T. Sukun, and F. Peng, "Breast tumour grading network based on adaptive fusion and microscopic imaging," *Opto-Electron. Eng.*, vol. 50, no. 1, 2023, Art. no. 220158.
- [8] Y. Wang, F. Luo, X. Yang, Q. Wang, Y. Sun, S. Tian, P. Feng, P. Huang, and H. Xiao, "The Swin-transformer network based on focal loss is used to identify images of pathological subtypes of lung adenocarcinoma with high similarity and class imbalance," *J. Cancer Res. Clin. Oncol.*, vol. 149, no. 11, pp. 8581–8592, Sep. 2023.

- [9] P. Huang, X. Tan, C. Chen, X. Lv, and Y. Li, "AF-SENet: Classification of cancer in cervical tissue pathological images based on fusing deep convolution features," *Sensors*, vol. 21, no. 1, p. 122, 2020.
- [10] C. Du, Y. Li, P. Xie, X. Zhang, B. Deng, G. Wang, Y. Hu, M. Wang, W. Deng, D. G. Armstrong, Y. Ma, and W. Deng, "The amputation and mortality of inpatients with diabetic foot ulceration in the COVID-19 pandemic and postpandemic era: A machine learning study," *Int. Wound J.*, vol. 19, no. 6, pp. 1289–1297, Oct. 2022.
- [11] O. Güley, S. Pati, and S. Bakas, "Classification of infection and ischemia in diabetic foot ulcers using VGG architectures," in *Diabetic Foot Ulcers Grand Challenge*. Cham, Switzerland: Springer, Sep. 2021, pp. 76–89.
- [12] J. Tulloch, R. Zamani, and M. Akrami, "Machine learning in the prevention, diagnosis and management of diabetic foot ulcers: A systematic review," *IEEE Access*, vol. 8, pp. 198977–199000, 2020.
- [13] W. Ren, A. H. Bashkandi, J. A. Jahanshahi, A. Q. M. AlHamad, D. Javaheri, and M. Mohammadi, "Brain tumor diagnosis using a step-by-step methodology based on courtship learning-based water strider algorithm," *Biomed. Signal Process. Control*, vol. 83, May 2023, Art. no. 104614.
- [14] B. Cassidy, N. D. Reeves, J. M. Pappachan, N. Ahmad, S. Haycocks, D. Gillespie, and M. H. Yap, "A cloud-based deep learning framework for remote detection of diabetic foot ulcers," *IEEE Pervasive Comput.*, vol. 21, no. 2, pp. 78–86, Apr. 2022.
- [15] K. Munadi, K. Saddami, M. Oktiana, R. Roslidar, K. Muchtar, M. Melinda, R. Muharar, M. Syukri, T. F. Abidin, and F. Arnia, "A deep learning method for early detection of diabetic foot using decision fusion and thermal images," *Appl. Sci.*, vol. 12, no. 15, p. 7524, Jul. 2022.
- [16] M. H. Alshayegi, S. C. Sindhu, and S. Abed, "Early detection of diabetic foot ulcers from thermal images using the bag of features technique," *Biomed. Signal Process. Control*, vol. 79, Jan. 2023, Art. no. 104143.
- [17] G. D'Angelo, D. Della-Morte, D. Pastore, G. Donadel, A. De Stefano, and F. Palmieri, "Identifying patterns in multiple biomarkers to diagnose diabetic foot using an explainable genetic programming-based approach," *Future Gener. Comput. Syst.*, vol. 140, pp. 138–150, Mar. 2023.
- [18] L. Alzubaidi, M. A. Fadhel, S. R. Oleiwi, O. Al-Shamma, and J. Zhang, "DFU\_QUtNet: Diabetic foot ulcer classification using novel deep convolutional neural network," *Multimedia Tools Appl.*, vol. 79, nos. 21–22, pp. 15655–15677, Jun. 2020.
- [19] M. Goyal, "Novel computerised techniques for recognition and analysis of diabetic foot ulcers," Ph.D. thesis, Manchester Metropolitan Univ., 2019. [Online]. Available: [https://e-space.mmu.ac.uk/625105/1/Thesis\\_Manu\\_Revised.pdf](https://e-space.mmu.ac.uk/625105/1/Thesis_Manu_Revised.pdf)
- [20] T. Arumuga Maria Devi and R. Hepzibai, "Clinical assessment of diabetic foot ulcers using GWO-CNN based hyperspectral image processing approach," *IETE J. Res.*, 2022, doi: [10.1080/03772063.2022.2099469](https://doi.org/10.1080/03772063.2022.2099469).
- [21] S. K. Das, P. Roy, and A. K. Mishra, "DFU\_SPNet: A stacked parallel convolution layers based CNN to improve diabetic foot ulcer classification," *ICT Exp.*, vol. 8, no. 2, pp. 271–275, Jun. 2022.
- [22] J. Amin, M. A. Anjum, A. Sharif, and M. I. Sharif, "A modified classical-quantum model for diabetic foot ulcer classification," *Intell. Decis. Technol.*, vol. 16, no. 1, pp. 23–28, Apr. 2022.
- [23] N. Al-Garaawi, R. Ebsim, A. F. H. Alharan, and M. H. Yap, "Diabetic foot ulcer classification using mapped binary patterns and convolutional neural networks," *Comput. Biol. Med.*, vol. 140, Jan. 2022, Art. no. 105055.
- [24] A. Oliveira, A. B. de Carvalho, and D. Dantas, "Faster R-CNN approach for diabetic foot ulcer detection," in *Proc. 16th Int. Joint Conf. Comput. Vis., Imag. Comput. Graph. Theory Appl.*, 2021, pp. 677–684.
- [25] C. Venkatesan, M. G. Sumithra, and M. Murugappan, "NFU-Net: An automated framework for the detection of neurotrophic foot ulcer using deep convolutional neural network," *Neural Process. Lett.*, vol. 54, no. 5, pp. 3705–3726, Oct. 2022.
- [26] C. A. Ferreira, T. Melo, P. Sousa, M. I. Meyer, E. Shakibapour, P. Costa, and A. Campilho, "Classification of breast cancer histology images through transfer learning using a pre-trained inception resnet v2," in *Proc. Int. Conf. Image Anal. Recognit.* Cham, Switzerland: Springer, May 2018, pp. 763–770.
- [27] P. Huang, P. He, S. Tian, M. Ma, P. Feng, H. Xiao, F. Mercaldo, A. Santone, and J. Qin, "A ViT-AMC network with adaptive model fusion and multiobjective optimization for interpretable laryngeal tumor grading from histopathological images," *IEEE Trans. Med. Imag.*, vol. 42, no. 1, pp. 15–28, Jan. 2023.
- [28] X. Zhou, C. Tang, P. Huang, S. Tian, F. Mercaldo, and A. Santone, "ASI-DBNet: An adaptive sparse interactive ResNet-vision transformer dual-branch network for the grading of brain cancer histopathological images," *Interdiscipl. Sci., Comput. Life Sci.*, vol. 15, no. 1, pp. 15–31, 2023, doi: [10.1007/s12539-022-00532-0](https://doi.org/10.1007/s12539-022-00532-0).
- [29] P. Huang, X. Zhou, P. He, P. Feng, S. Tian, Y. Sun, F. Mercaldo, A. Santone, J. Qin, and H. Xiao, "Interpretable laryngeal tumor grading of histopathological images via depth domain adaptive network with integration gradient CAM and priori experience-guided attention," *Comput. Biol. Med.*, vol. 154, Mar. 2023, Art. no. 106447.
- [30] X. Zhou, C. Tang, P. Huang, F. Mercaldo, A. Santone, and Y. Shao, "LPCANet: Classification of laryngeal cancer histopathological images using a CNN with position attention and channel attention mechanisms," *Interdiscipl. Sci., Comput. Life Sci.*, vol. 13, no. 4, pp. 666–682, Dec. 2021.
- [31] P. Huang, X. Tan, X. Zhou, S. Liu, F. Mercaldo, and A. Santone, "FABNet: Fusion attention block and transfer learning for laryngeal cancer tumor grading in P63 IHC histopathology images," *IEEE J. Biomed. Health Informat.*, vol. 26, no. 4, pp. 1696–1707, Apr. 2022.
- [32] Y. Guo, D. Yang, Y. Zhang, L. Wang, and K. Wang, "Online estimation of SOH for lithium-ion battery based on SSA-elman neural network," *Protection Control Mod. Power Syst.*, vol. 7, no. 1, pp. 1–17, Dec. 2022.
- [33] B. Li, S. Liang, D. Chen, and X. Li, "A decision-making method for air combat maneuver based on hybrid deep learning network," *Chin. J. Electron.*, vol. 31, no. 1, pp. 107–115, Jan. 2022.
- [34] *Diabetic Foot Ulcer (DFU)*. Accessed: Jul. 14, 2023. [Online]. Available: <https://www.kaggle.com/datasets/laithij/diabetic-foot-ulcer-dfu>
- [35] P. N. Thotad, G. R. Bharamagoudar, and B. S. Anami, "Diabetic foot ulcer detection using deep learning approaches," *Sensors Int.*, vol. 4, Jan. 2023, Art. no. 100210.



**SUNNAM NAGARAJU** received the B.Tech. degree from JNTUH, Hyderabad, in 2007, and the M.Tech. degree from NIT, Trichy, Tamil Nadu. He was an Assistant Professor with Lovely Professional University, Jalandhar, Punjab, India, from 2010 to 2016. He was also a Plant Engineer with OCTL, Hyderabad. He is currently an Associate Professor with MLRIT, Hyderabad, in 2010.



**KOLLATI VIJAYA KUMAR** received the Ph.D. degree in computer science and engineering from Karpagam University, Coimbatore. He has 15 years of teaching experience. He is currently an Associate Professor with the Department of CSE, GITAM School of Technology, GITAM University, Visakhapatnam, Andhra Pradesh, India. He has published 24 articles in international journals. His research interests include wireless networking, big data, data analytics, network security, cloud computing, and information security.

**B. PRAMEELA RANI** received the B.Tech. degree from the Aditya College of Engineering and Technology (ACET), Surampalem, in 2014, and the M.Tech. degree from the Aditya College of Engineering (Autonomous), Surampalem. She is currently an Assistant Professor with the Aditya College of Engineering. She was an Instructor in engineering colleges, from 2014 to 2021, on various technologies. Her current research interests include machine learning models and deep learning mechanisms.



**E. LAXMI LYDIA** is currently a Professor in computer science engineering with GMRIT. She is also a Big Data Analytics Online Trainer with the International Training Organization. She has presented various webinars on big data analytics. She is also with the Government DST Funded Project. She is also certified by the Microsoft Certified Solution Developer (MCSD). She is the author of the *Big Data Analytics* book. She holds a patent. She has published ten research papers in international conference proceedings. She has published more than 100 research articles in international journals in *Big Data Analytics* and *Data Science Journal*.



**MOHAMAD KHAIRI ISHAK** received the B.Eng. degree in electrical and electronics engineering from International Islamic University Malaysia (IIUM), Malaysia, the M.Sc. degree in embedded system from the University of Essex, U.K., and the Ph.D. degree from the University of Bristol, U.K. He is currently a Registered Graduate Engineer with the Board of Engineers Malaysia (BEM). He is also a Senior Lecturer in mechatronics engineering with the School of Electrical and Electronic Engineering, Universiti Sains Malaysia (USM). His background includes outstanding teaching experience with Universiti Sains Malaysia, instructing students to stimulate engineering information interest and retention while invigorating classes through the use of new technologies and models. His research interests include embedded systems, real-time control communications, and Internet of Things (IoT). Emphasis is given toward the development of theoretical and practical methods which can be practically validated. Recently, significant research effort has been directed toward important industrial issues of embedded networked control systems and IoT.

**IMEN FILALI** received the master's degree in networks and distributed systems and the Ph.D. degree from the University of Nice Sophia-Antipolis, France, in 2007 and 2011, respectively. She has been an Assistant Professor with the National Engineering School of Gabes, Tunisia, since 2011. From December 2014 to September 2015, she was a Postdoctoral Researcher with the Swiss Federal Institute of Technology of Lausanne (EPFL) working within the Distributed Information Systems Laboratory (LSIR). Since January 2018, she has been with the Department of Computer Science, College of Computer and Information Sciences, Princess Nourah Bint Abdulrahman University, as an Assistant Professor. Her main research interests include cloud computing, big data analytics, artificial intelligence, and computer vision.

**FATEN KHALID KARIM** received the Ph.D. degree in computing and information technology from Flinders University, SA, Australia. She is currently an Assistant Professor with the Department of Computer Sciences, College of Computer and Information Sciences, Princess Nourah Bint Abdulrahman University, Riyadh, Saudi Arabia. Her research interests include cloud computing and information technology. She has published several research articles in her field.



**SAMIH M. MOSTAFA** received the bachelor's and M.Sc. degrees in computer science from the Computer Science-Mathematics Department, Faculty of Science, South Valley University, in 2004 and 2010, respectively, and the Ph.D. degree in computer science from the Advanced Information Technology Department, Graduate School of Information Technology, Kyushu University, Japan, in 2017. His research interests include machine learning and CPU scheduling. He is currently a fellow of the Academy of Scientific Research and Technology (ASRT), Egypt.

...